

***In situ* measurements of stress evolution for nanotwin formation during pulse electrodeposition of copper**

Di Xu,^{1,a)} Vinay Sriram,¹ Vidvuds Ozolins,¹ Jenn-Ming Yang,¹ K. N. Tu,¹ Gery R. Stafford,² and Carlos Beauchamp²

¹*Department of Materials Science and Engineering, University of California at Los Angeles, Los Angeles, California 90095-1595, USA*

²*National Institute of Standards and Technology, Gaithersburg, Maryland, USA*

(Received 8 October 2008; accepted 4 December 2008; published online 28 January 2009)

In situ stress measurements were performed during high frequency pulse electrodeposition of nanotwinned Cu thin films. Periodic stress changes during pulse-on and pulse-off periods were observed. The stress profile showed an abrupt increase in tensile stress to about 400 MPa during the pulse-on period and a stress relaxation during the pulse-off period. First-principles calculations predict that a complete relaxation of the tensile stress allows the formation of nanotwins separated by 28 nm or more. This is in good agreement with the results obtained from microstructural analysis of the Cu films fabricated during *in situ* stress measurements. © 2009 American Institute of Physics. [DOI: 10.1063/1.3068191]

I. INTRODUCTION

A high density of nanotwins in Cu has been shown to improve the mechanical strength and maintain the good ductility and electrical conductivity of Cu.¹ It has been suggested that the formation of nanotwins in Cu depends on the stress evolution and relaxation during pulse electrodeposition.² Stress evolution during the deposition of thin metal films has been studied extensively because it plays a very important role in the kinetics of film growth.^{3–16} Most studies have shown that the stress evolution follows the compression-tension-compression (CTC) transition, which is typical for Cu deposition by electroplating and vapor deposition techniques.^{11–16} The initial compressive stress occurs in the discrete-nuclei stage of growth and is due to the surface stress of these small particles. The rapid development of tensile stress is associated with nuclei coalescence and grain boundary formation while the final compressive stage occurs during thickening of the continuous film. Electrodeposition of Cu has been an important metallization process in microelectronics technology, e.g., it is used to produce the damascene interconnect structure. Upon decreasing the device feature sizes, the stresses may become significant in Cu interconnect pads, lines, and vias.

Stress evolution in electrodeposition processes using pulse signal is of special interest since this method leads to smoother surfaces, higher densities of twin boundaries in Cu, and reduced void formation in comparison with the traditional direct current (dc) plating. Recently, high density nanoscale twin boundaries in polycrystalline Cu have attracted great interest^{1,2,17–23} because they bring about the highly desirable combination of high mechanical strength and good electrical conductivity. The formation mechanism of high density nanotwins has been studied extensively. Our previous first-principles calculations of the energetics of nanotwin formation suggest that stress relaxation plays a key

role in nanotwin formation since a highly strained face-centered-cubic (FCC) Cu is energetically less stable than a strain-relaxed nanotwinned Cu.² Direct experimental investigation of the stress evolution is necessary to prove that stress generation and stress relaxation occur during the formation of nanotwinned Cu.

Several *in situ* techniques have been developed that measure residual stress during electrochemical processing.^{10,11} The simplest and most widely used methods involve the measurement of the deflection of a flexible cathode, typically in a direction that is perpendicular to the in-plane stress generated in the film. Fairly sophisticated methods for tracking this deflection have been developed in the past 20 years; the more popular make use of capacitance measurements, laser beam reflection, and scanning tunneling microscopy/atomic force microscopy. Previous studies by Kongstein and co-workers^{11,12} showed stress relaxation when dc electrodeposition of Cu films was interrupted to open circuit for 15 min. In this study, we report *in situ* stress measurements of the stress evolution during the pulse electrodeposition process, which produces nanotwins in Cu.

II. EXPERIMENTAL

The *in situ* stress measurement system consists of an electrochemical cell, an optical system which can detect with high sensitivity the bending of the cantilever beam on which the Cu film is being deposited, and a signal processing unit. The light source was a 1 mW helium-neon laser (JDS Uniphase, model 1108P). The laser beam reflected by the bending cantilever passes through a beam splitter and is detected by a duo-lateral position sensitive detector (PSD) with dimensions of 20 × 20 mm² (DLS-20 from UTD Sensors Inc.). The PSD output is amplified, measured by a National Instrument analog to digital card and then transferred to a Macintosh Power personal computer. The signal is then converted into vertical and horizontal positions on the PSD, which can be used for stress calculations. More details of the

^{a)}Electronic mail: dixu@ucla.edu.

experimental setup can be found in Refs. 11 and 12.

The cantilever was a borosilicate glass strip (D 263, Schott) measuring $60 \times 3 \times 0.108 \text{ mm}^3$. The glass had a Young's modulus of $72.9 \times 10^9 \text{ N m}^{-2}$ and a Poisson ratio of 0.208. Onto one side of the cantilever a 4 nm thick adhesion layer of titanium and a subsequent 250 nm film of gold were vapor deposited by electron-beam evaporation. Prior to use, the electrodes were cleaned in piranha solution (3:1 volume mixture of concentrated H_2SO_4 :30% H_2O_2). The Au electrodes had a strong (111) crystallographic orientation. The 200 reflection was not apparent in θ -2 θ x-ray scans and rocking curves of the 111 reflection generally yielded a full width at half maximum on the order of 2° . These films have a fiber texture, i.e., there is no in-plane orientation.

The electrochemical cell was a single compartment Pyrex cell covered by a perfluoroethylene cap. A glass disk was joined to the back of the cell to allow it to be held and positioned by a standard mirror mounted on the optical bench. Copper foil served as the counterelectrode while a Cu wire served as the reference electrode. The electrolyte used in the study was 0.25 mol/l CuSO_4 and 1.0 mol/l H_2SO_4 and pulse current was achieved using an EG&G Princeton Applied Research Corp. model 273 potentiostat/galvanostat. After the *in situ* stress measurements, microstructural analysis of the Cu films was carried out by x-ray diffraction (XRD), scanning electron microscopy (SEM), focused ion beam (FIB), and transmission electron microscopy (TEM).

The relationship between the force per cantilever beam width F_w exerted by processes occurring on the electrode surface and the radius of curvature of the cantilever is given by Stoney's equation,

$$F_w = \frac{Y_s t_s^2}{6(1 - \nu_s)R} = \int_0^{t_f} \sigma_f dt, \quad (1)$$

where Y_s , ν_s , and t_s are Young's modulus, Poisson's ratio, and thickness of the glass substrate, respectively, and R is the radius of curvature of the cantilever. When the force on the cantilever is the result of bulk metal deposition, F_w is equal to the stress \times thickness product, i.e., the film stress σ_f integrated through the thickness of the film, t_f [Eq. (1)]. We report the cantilever data as both the stress \times thickness product (which we will refer to as the "stress \times thickness") and the average film stress (σ_{av}), defined as F_w divided by the film thickness (t_f) as shown in Eq. (2),

$$\sigma_{av} = \frac{F_w}{t_f}. \quad (2)$$

In all cases the film thickness was calculated from the charge, assuming 100% current efficiency and uniform current distribution.

III. RESULTS

We performed measurements of *in situ* stress during dc electrodeposition and pulsed electrodeposition using the same average current density. The dc density was 10 mA/cm² and the pulse current was 110 mA/cm² with 5 ms pulse-on time and 50 ms pulse-off time periods. Figure 1 shows the average stress evolution curves for dc plating and

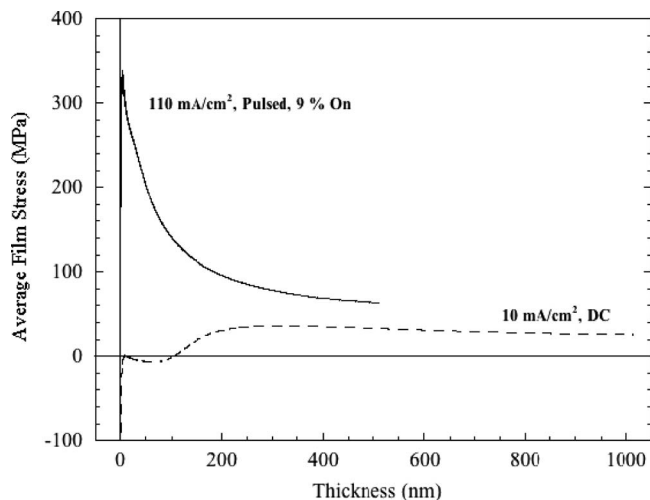


FIG. 1. Average stress evolution as a function of film thickness for two electrodeposition processes of Cu on glass/Au substrates with the same average current density: pulse electrodeposition with 110 mA/cm² pulse current, 5 ms pulse-on time and 50 ms pulse-off time (solid line), and dc electrodeposition with 10 mA/cm² current density (dashed line). The pulsed deposit was stopped at a thickness of 500 nm.

pulse plating with the same average current density. The stress response for the dc deposit is very similar to that reported for potentiostatic deposition¹¹ except that the initial stage of compressive stress, which has been attributed to the surface stress associated with small nuclei, is extended to larger nominal thicknesses. This is likely due to the nature of galvanostatic deposition and the additional time required for double layer charging and reaching the overpotential required for nucleation. This overall stress response is typical for deposition at small overpotentials. In contrast, the stress of the pulsed deposit becomes tensile quite quickly presumably because of the much higher applied deposition current. This results in a significantly higher nucleation density and nuclei coalescence at very small nominal thickness. A maximum tensile stress of 340 MPa was achieved at a thickness of approximately 6 nm. Much of this tensile stress disappears by the time the film reaches a thickness of 200 nm. There is some debate in the literature as to whether this is due to relaxation processes or simultaneous growth processes that generate compressive stress.¹⁴⁻¹⁶ However, in our case, the decrease in tensile stress is more likely due to stress relaxation based on further detailed observation during both pulse-on and pulse-off deposition times. In the case of dc electroplating with the same average current density, the maximum tensile stress was less than 50 MPa at 250 nm thickness. The tensile stress decreased very slowly as the deposit thickened.

First-principles calculations of nanotwinned Cu and FCC Cu suggest that stress relaxation is the driving force for nanotwin formation.² Figure 1 indicates that pulse electroplating can provide a larger driving force (i.e., elastic strain energy) for nanotwin formation than dc plating with the same average current density. Microstructural observations of the dc plated Cu film show very little twin formation.

In order to observe the stress evolution during both the on and off time periods during pulse electroplating, faster data acquisition was employed. The deposition was con-

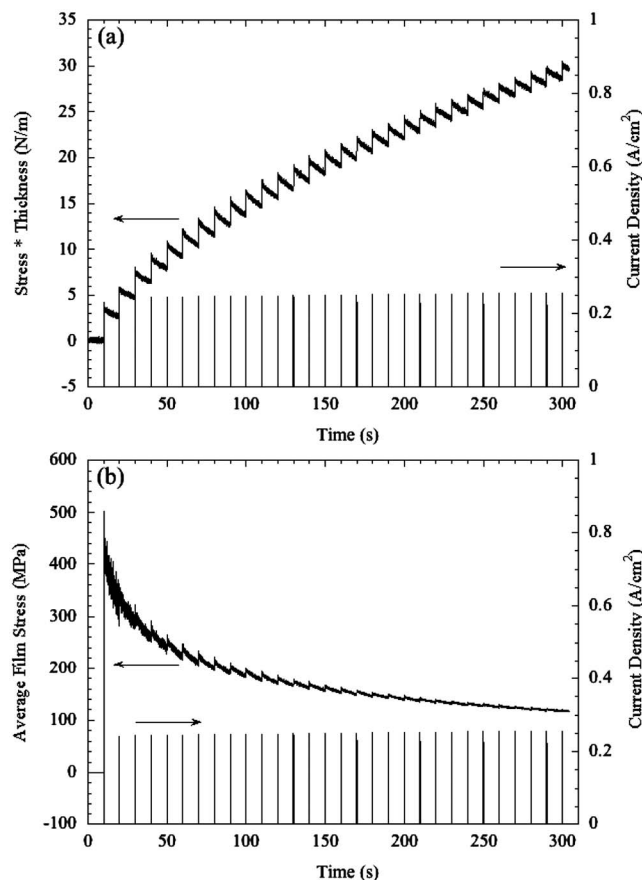


FIG. 2. The evolution of (a) deposit stress thickness and (b) average film stress as a function of pulse deposition time. The deposition potential was -0.70 V vs Cu with 0.1 s pulse-on time and 9.9 s pulse-off time.

trolled potentiostatically using a pulse potential of -0.7 V versus Cu, resulting in a pulse current density of about 0.22 A/cm². The pulse-on time was 0.1 s with 1% duty cycle (9.9 s off time). The nominal film thickness produced by a single pulse was 8.2 nm based on the deposition charge. The laser position response was recorded every 1 ms during the pulse deposition, allowing us to measure the stress thickness and the average film stress during each pulse-on and pulse-off deposition periods. Figure 2 shows the stress thickness and the average film stress as a function of the deposition time. The stress thickness evolves with a periodicity that is consistent with the pulse current cycles. During the on time period, the stress thickness moves in the tensile direction whereas during the off cycle, approximately 60% of this is relaxed. The maximum tensile stress recorded was 400 MPa at a film thickness of 10 nm. Interestingly, the stress relaxation observed during each off cycle is a miniature version of the overall stress response, i.e., high tensile stress followed by partial relaxation.

We examined two different pulsing conditions to determine the generality of this tensile stress generation and relaxation. The stress thickness and average biaxial stress for different on-off times are plotted in Fig. 3. The average biaxial stress, Fig. 3(b), is plotted as a function of deposit thickness rather than time so that the influence of pulsing conditions on the stress for a given thickness could be evaluated. In both cases, tensile stress is generated during the

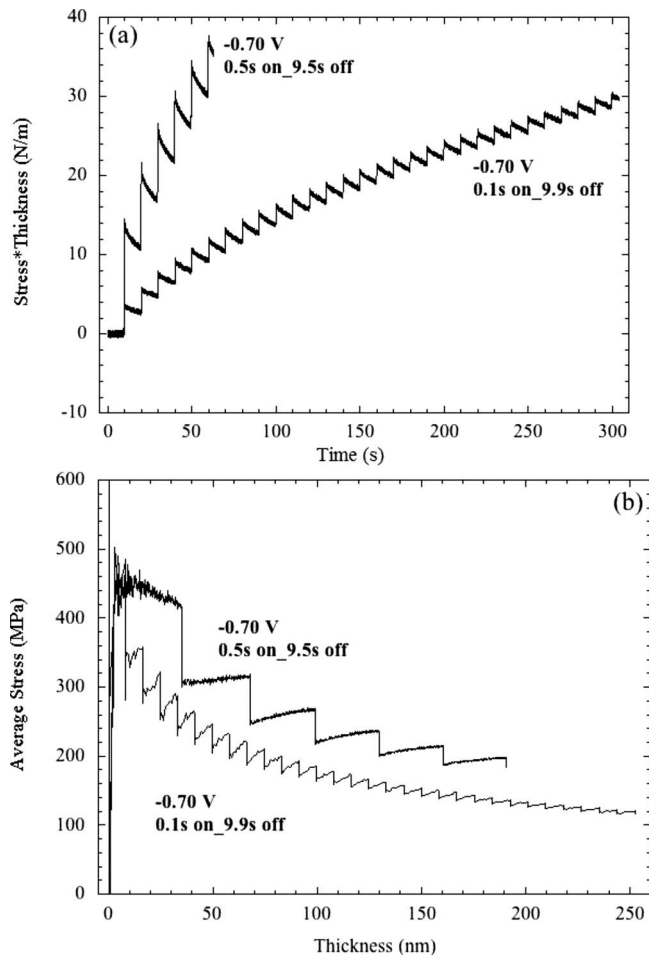


FIG. 3. The evolution of (a) deposit stress thickness as a function of time and (b) average film stress as a function of deposit thickness for pulse-on times of 0.1 and 0.5 s.

pulse-on time, followed by relaxation during the pulse-off time. The faster increase in stress thickness for the large on-time condition simply reflects the longer growth time and more rapidly increasing thickness. When the stress thickness is divided by the thickness to reveal the average stress, the curves have similar shape. It is readily apparent, however, that a smaller pulse-on time results in smaller tensile stress, suggesting that relaxation is linked to the amount of material deposited during the growth cycle. This is clearly seen in Fig. 3(b) in that the stress generated in the first pulse is identical for the two deposits. The departure occurs during the first relaxation cycle. We believe that this stress relaxation is related to nanotwin formation in the Cu films during pulse electrodeposition. It should be noted that the tensile stress and the extent of stress relaxation depend on both the pulse-on and pulse-off periods, as well as the potential of the pulse. The pulse electrodeposition conditions shown in Fig. 3 only give a general trend of stress evolution which drives the growth of twins but are not sufficient to make a quantitative dependence of twin density on pulse plating conditions.

XRD, SEM, and TEM observations were performed to characterize the microstructure of the pulse electroplated Cu film (stress response shown in Fig. 2). The film is polycrystalline Cu with no strong preferred grain orientation, which means that $\{111\}$ twin boundaries may form in different ori-

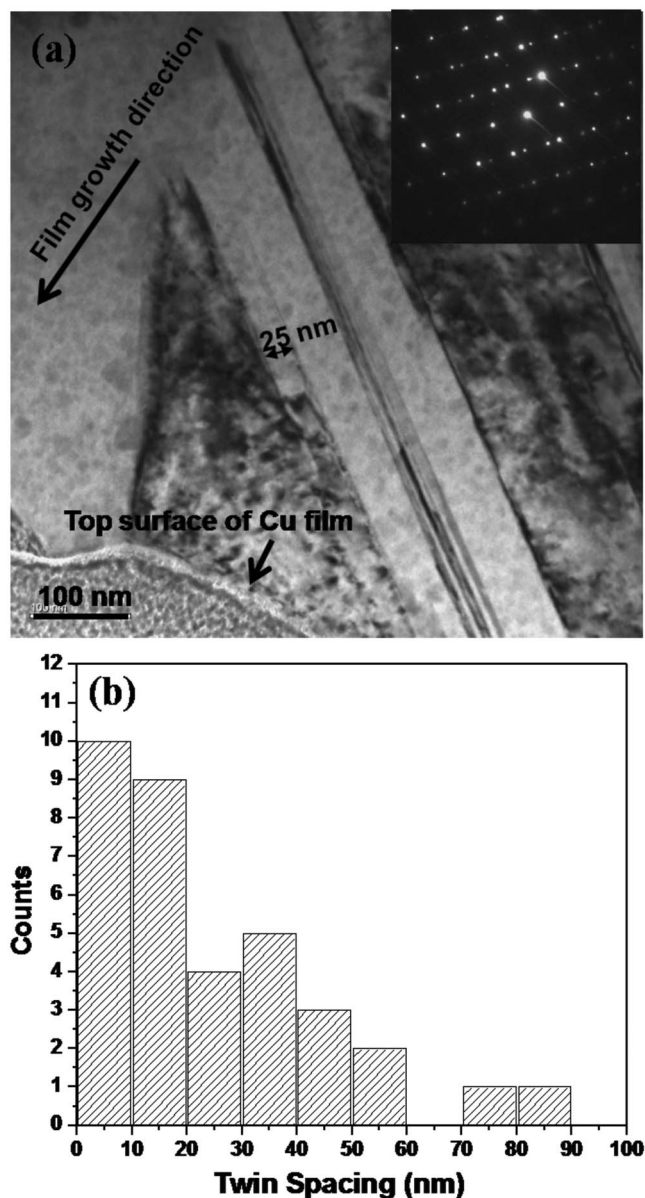


FIG. 4. (a) TEM Bright field image of Cu grains containing nanoscale twin boundaries from the sample deposited during *in situ* stress measurements (-0.70 V pulse potential, 0.1 s pulse-on time, and 9.9 s pulse-off time), diffraction patterns of the Cu grains showing twinning spots. The growth direction and the top of the Cu film are indicated with arrows. (b) Histogram of twin spacing for the Cu film sample deposited during *in situ* stress measurements.

entation angles with respect to the plane of the film. Cross sections of the film were prepared by FIB. Figure 4(a) shows a TEM bright field image of Cu grains in which nanoscale twins are clearly visible. The direction along which the film grew is indicated in the figure. The crystal orientation of the selected grain perpendicular to the cross section is $[011]$. The accompanying diffraction pattern also shows diffraction spots caused by twinning. A larger area containing twin boundaries was examined and a histogram of twin spacing is presented in Fig. 4(b) based on these observations. The average twin spacing is approximately 10 – 20 nm.

IV. DISCUSSION

Stress relaxation is a common occurrence during film deposition and different relaxation mechanisms have been

proposed in the literature.^{14–16,24–28} Much of this effort has focused on the relaxation of compressive stress that has been widely observed during the thickening stage of film growth.^{8,16,25} Film deposition, from both electrolyte and the gas phase, is a nonequilibrium solidification process. As a consequence, these models consider the nonequilibrium nature of the surface and the role of the adatom population on the stress state of the film. They argue that compressive stress can be generated by the presence of a nonequilibrium population of adatoms, either directly due to surface stress^{8,26} or by driving adatoms into the grain boundaries.^{16,25} Both models predict stress relaxation when deposition is interrupted. Although not directly applicable to the situation presented here for pulsed deposition where tensile stress is generated, the idea that the high current density used during the growth pulse creates a nonequilibrium state in the Cu that relaxes during the off cycle does indeed have merit.

The relaxation of tensile stress has been addressed to a lesser extent. Surface diffusion has been proposed as a mechanism for relieving tensile stresses generated by island coalescence. Adatoms on the free surface of the film have a fast diffusion path down to the grain boundary, a process analogous with Coble creep in bulk polycrystals.^{14,15,27,28} However, stress relaxation by this mechanism, though active during island coalescence, is suppressed once the film becomes continuous. During the pulse deposition presented here, approximately 10 nm of fresh Cu is deposited during each pulse cycle. Due to the high current densities applied, newly deposited grains nucleate and coalesce while some existing grains grow. As a consequence, it is likely that some of the strain energy generated during the pulse will be relaxed by surface diffusion. Although the data in Fig. 2 have a 10 s off time, this is not required for twin formation but was simply used to highlight the relaxation transient. Typical off times, such as the Fig. 1 data, are 50 ms. If we use surface diffusivity of Cu at room temperature²⁹ as 2×10^{-15} cm^2/s and assuming a diffusion distance of $(Dt)^{1/2}$, a diffusion distance of only about 0.1 nm will be obtained. Therefore, during this short off time, relaxation processes controlled by surface diffusion will be very limited. Even in solution, where surface diffusion may be expected to be somewhat faster, relaxation through surface diffusion processes is expected to play a minor role.

An additional relaxation mechanism has been proposed for heteroepitaxial film growth where misfit strain is introduced. It has been argued that when the mismatch strain is larger than a critical value and the twin boundary is small enough, the formation of misfit twinning can be more dominant than the formation of dislocations for strain relaxation.^{24,30} Although the nanoscale twins formed in the Cu films made by pulse deposition are growth twins, not misfit twins, stress relaxation may still be associated with twin formation.

From an energetic point of view, our earlier first-principles calculations of the total energies have shown that stress-relaxed nanotwin Cu is energetically more stable than a highly stressed FCC Cu. During the pulse-on time of electroplating, the high current density generates a high density of Cu nuclei, which subsequently coalesce and thus increase

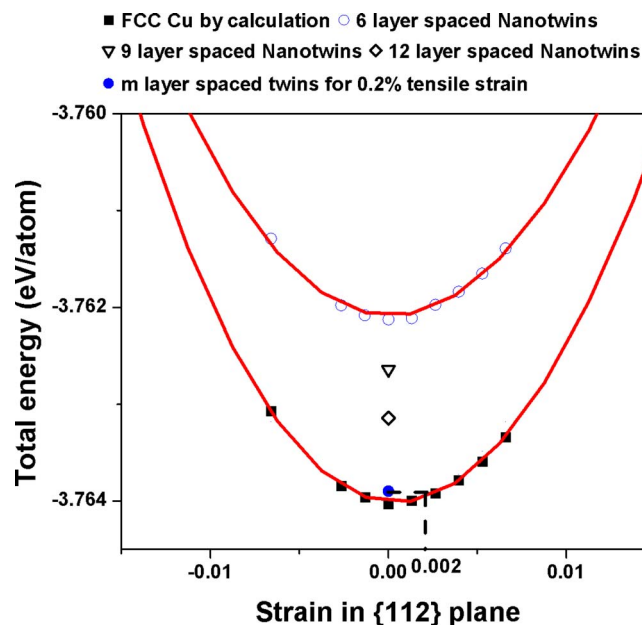


FIG. 5. (Color online) Total energy of FCC Cu and nanotwinned Cu as a function of strain. The total energies of nanotwinned Cu with 6 (111) layers, 9 (111) layers, and 12 (111) layers at strain-free states are indicated in the figure. The dashed lines show that if 0.2% tensile strain in FCC Cu is fully relieved, the possible nanotwin structure with the same energy will be the spot which is marked as m layer spacing. The spacing can be calculated as 135 (111) layers, which is about 28 nm.

the tensile stress in the film. The subsequent pulse-off period allows the rearrangement of Cu clusters by recrystallization so that stress relaxation can occur through formation of twin boundaries. It is important to distinguish this loss of tensile stress from that which is observed for CTC stress evolution during Cu deposition. In traditional CTC, the tensile stress decreases due to the simultaneous generation of compressive growth stress, most likely the result of incorporation of Cu adatoms into grain boundaries.¹⁶ When deposition is interrupted, relaxation occurs in the tensile direction. During the off cycle in pulse deposition, growth stress is not generated but the existing stresses are given time to relax. Here, we attribute the decrease in tensile stress to the formation of nanotwins in the pulse-off period when no more material is being deposited.

In order to verify how strongly the stress generation and relaxation is related to the twin formation, the possible nanotwin spacing has been calculated from the stress value and compared to the TEM observation. The expected minimum separation between twin boundaries can be calculated by assuming a given stress introduced by the pulse current and complete stress relaxation during the pulse-off period. During a pulse cycle of 10 s used in Fig. 2, a tensile force of about 3.2 N/m was repeatedly generated. Using a biaxial modulus for Cu of 198 GPa, the induced in-plane strain of the newly deposited 8 nm Cu in a single pulse cycle is 0.2%. In Ref. 2 it was found that a complete relaxation of a tensile strain of 1.1% gives a minimum nanotwin spacing of 1.3 nm. This critical twin spacing can be obtained by equating the total energy of the strained FCC Cu to that of the strain-relaxed nanotwin Cu, as shown in Fig. 5. We use the strain-energy curve with {112} strained plane because for Cu crystal

with {111} twin boundaries, $\langle 112 \rangle$ and $\langle 011 \rangle$ are the grain orientations which make twin boundaries and twin spacing visible, as shown in Fig. 4. From the same curve, we can locate the total energy of 0.2% tensile strained FCC Cu and calculate the possible twin spacing from the following equation:

$$E(m) = E_{\text{FCC}} + \frac{\gamma_{\text{twin}} A}{m} \leq E \quad (\varepsilon = 0.2\%), \quad (3)$$

where $E(m)$ is the total energy of Cu with m (111) atomic layers separating twin boundaries, E_{FCC} is the energy of strain free FCC Cu, γ_{twin} is the twin boundary energy, and A is the unit surface area of a twin boundary. The twin thickness, calculated from the number of (111) layers between two twin planes, is about 28 nm for 0.2% tensile strain. We note that the tensile force is not completely relaxed after every pulse-off period, and that there is still a small residual tensile stress at the end of each deposition cycle. Thus, the twin thickness should be slightly larger than the critical value calculated above. This is in reasonable agreement with the results in the TEM characterization, demonstrating that pulse-deposition-induced high stress and subsequent stress relaxation indeed play an important role in the mechanism of nanotwin formation.

V. SUMMARY

In situ stress measurements were performed for pulse electrodeposition of Cu. Stress evolutions during each period of 0.1 s pulse-on time and 9.9 s pulse-off time were detected. It was found that periodic increase in tensile stress and stress relaxation took place during the pulse-on time and pulse-off time, respectively. Using the measured average stress, the twin spacing can be predicted by first-principles calculations and shown to be approximately 28 nm, which is consistent with the observed twin dimension by TEM microstructure characterization. We propose that stress relaxation in the pulse-off periods is a consequence of nanotwin formation during pulse electrodeposition.

ACKNOWLEDGMENTS

The UCLA authors greatly acknowledge the support by NSF/NIRT Contract No. CMS-0506841. V.O. acknowledges financial support from the NSF ITR program under Grant No. DMR-0427638 and by the FCRP Center for Functional Engineered NanoArchitectonics (FENA). V.S. acknowledges the National Center for Electron Microscopy which is supported by the Scientific User Facilities Division of the Office of Basic Energy Sciences, U.S. Department of Energy under Contract No. DE-AC02-05CH11231 for TEM sample preparation. Certain trade names are mentioned for experimental information only. In no case does it imply a recommendation or endorsement by NIST.

¹L. Lu, Y. F. Shen, X. H. Chen, L. H. Qian, and K. Lu, *Science* **304**, 422 (2004).

²D. Xu, W. L. Kwan, K. Chen, X. Zhang, V. Ozolins, and K. N. Tu, *Appl. Phys. Lett.* **91**, 254105 (2007).

³R. Abermann, *Vacuum* **41**, 1279 (1990).

⁴A. L. Shull and F. Spaepen, *J. Appl. Phys.* **80**, 6243 (1996).

- ⁵R. Koch, *J. Phys.: Condens. Matter* **6**, 9519 (1994).
- ⁶W. D. Nix and B. M. Clemens, *J. Mater. Res.* **14**, 3467 (1999).
- ⁷F. Spaepen, *Acta Mater.* **48**, 31 (2000).
- ⁸C. Friesen, S. C. Seel, and C. V. Thompson, *J. Appl. Phys.* **95**, 1011 (2004).
- ⁹W. Haiss, R. J. Nichols, and J. K. Sass, *Surf. Sci.* **388**, 141 (1997).
- ¹⁰R. Weil, *Plating* **58**, 137 (1971); R. Weil, *ibid.* **57**, 1231 (1970); R. Weil, *ibid.* **58**, 50 (1971).
- ¹¹O. E. Kongstein, U. Bertocci, and G. R. Stafford, *J. Electrochem. Soc.* **152**, C116 (2005).
- ¹²G. R. Stafford, O. E. Kongstein, and C. R. Beauchamp, *ECS Trans.* **2**, 185 (2007).
- ¹³S. Ahmed, T. T. Ahmed, M. O'Grady, S. Nakahara, and D. N. Buckley, *J. Appl. Phys.* **103**, 073506 (2008).
- ¹⁴S. C. Seel, C. V. Thompson, S. J. Hearne, and J. A. Floro, *J. Appl. Phys.* **88**, 7079 (2000).
- ¹⁵J. A. Floro, S. J. Hearne, J. A. Hunter, P. Kotula, E. Chason, S. C. Seel, and C. V. Thompson, *J. Appl. Phys.* **89**, 4886 (2001).
- ¹⁶J. A. Floro, E. Chason, R. C. Cammarata, and D. J. Srolovitz, *MRS Bull.* **27**, 19 (2002).
- ¹⁷E. Ma, Y. M. Wang, Q. H. Lu, M. L. Sui, L. Lu, and K. Lu, *Appl. Phys. Lett.* **85**, 4932 (2004); L. Lu, R. Schwaiger, Z. W. Shan, M. Dao, K. Lu, and S. Suresh, *Acta Mater.* **53**, 2169 (2005).
- ¹⁸Y. F. Shen, L. Lu, Q. H. Lu, Z. H. Jin, and K. Lu, *Scr. Mater.* **52**, 989 (2005).
- ¹⁹L. H. Xu, P. Dixit, J. M. Miao, H. L. Pang, X. Zhang, K. N. Tu, and R. Preisser, *Appl. Phys. Lett.* **90**, 033111 (2007).
- ²⁰X. Zhang, K. N. Tu, Z. Chen, Y. K. Tan, C. C. Wong, S. G. Mhaisalkar, X. M. Li, C. H. Tung, and C. K. Cheng, *J. Nanosci. Nanotechnol.* **8**, 1 (2007).
- ²¹X. Zhang, H. Wang, X. H. Chen, L. Lu, K. Lu, R. G. Hoagland, and A. Misra, *Appl. Phys. Lett.* **88**, 173116 (2006).
- ²²A. M. Hodge, Y. M. Wang, and T. W. Barbee, *Mater. Sci. Eng., A* **429**, 272 (2006).
- ²³X. Zhang, A. Misra, H. Wang, T. D. Shen, M. Nastasi, T. E. Mitchell, J. P. Hirth, R. G. Hoagland, and J. D. Embury, *Acta Mater.* **52**, 995 (2004).
- ²⁴L. L. Liu, Y. S. Zhang, and T. Y. Zhang, *J. Appl. Phys.* **101**, 063501 (2007); Y. S. Zhang, L. L. Liu, and T. Y. Zhang, *ibid.* **101**, 063502 (2007).
- ²⁵E. Chason, B. W. Sheldon, L. B. Freund, J. A. Floro, and S. J. Hearne, *Phys. Rev. Lett.* **88**, 156103 (2002).
- ²⁶C. Friesen and C. V. Thompson, *Phys. Rev. Lett.* **89**, 126103 (2002).
- ²⁷M. D. Thouless, *Acta Metall. Mater.* **41**, 1057 (1993).
- ²⁸M. Kobrinsky and C. V. Thompson, *Appl. Phys. Lett.* **73**, 2429 (1998).
- ²⁹K. N. Tu, *J. Appl. Phys.* **94**, 5451 (2003).
- ³⁰M. Dynna, A. Marty, B. Gilles, and G. G. Patrat, *Acta Mater.* **45**, 257 (1997).